

Photoinduced effects in the vicinity of the smectic-A-smectic- C_A^* transition: Polarization, tilt angle, and response time studies

Geetha G. Nair,¹ Gurumurthy Hegde,¹ S. Krishna Prasad,¹ Chethan V. Lobo,¹ and Y. S. Negi²

¹Centre for Liquid Crystal Research, Jalahalli, Bangalore 560 013, India

²Centre for Materials for Electronics Technology, Panchwati, Off Pashan Road, Pune 411 008, India

(Received 13 April 2005; revised manuscript received 31 October 2005; published 30 January 2006)

We report detailed measurements of the photoinduced effects on the electric polarization, tilt angle, response time, and rotational viscosity in the vicinity of the smectic-A–antiferroelectric-smectic-C (Sm- C_A^*) transition of a guest-host system consisting of photoactive azobenzene-based guest molecules and nonphotoactive host molecules. In the Sm- C_A^* phase all the parameters, except the tilt angle, exhibit both the primary and secondary photoferroelectric effects. The tilt angle dependence of the polarization in the absence of light and in light-on conditions have been analyzed in terms of the predictions of the generalized mean-field and microscopic models.

DOI: 10.1103/PhysRevE.73.011712

PACS number(s): 61.30.-v, 42.70.Gi, 64.70.Md

I. INTRODUCTION

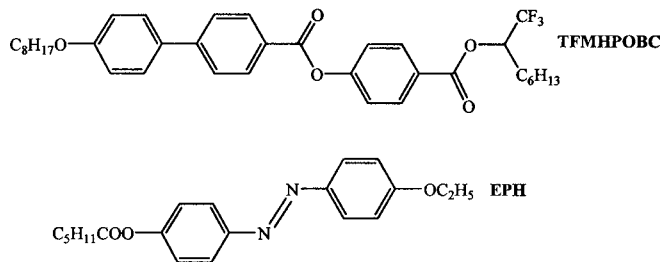
Smectic-A (Sm-A) and smectic-C (Sm-C) liquid crystals are fluid phases in which the rodlike liquid crystalline molecules orient, on average, along a common direction, referred to as the director, and are stacked in layers with the director aligned either along (Sm-A) or at an angle to (Sm-C) the layer normal [1]. If the system is comprised of chiral molecules, in the chiral Sm-C (Sm- C^*) phase the chirality imposes a precession of the tilting direction from one layer to the next, leading to a macroscopic helix. A more important consequence of the chirality is to lower the symmetry of the phase leading to the appearance of ferroelectricity in the Sm- C^* phase [2]. In 1989, a variant of this phase, known as the antiferroelectric Sm- C^* or Sm- C_A^* phase, was reported in which the molecules in neighboring layers are tilted from the smectic layer normal in almost opposite directions [3]. More recently, other variants like the smectic C_γ^* and smectic- C_α^* (Sm- C_α^*) phases have also been reported [4]. Generally, the Sm- C^* phase intervenes between the Sm-A and Sm- C_A^* phases. But in certain materials there can be a direct transition from the Sm-A to the Sm- C_A^* phase.

The phenomenon of reversible photoinduced shape transformation of chromophoric molecules, such as azobenzenes, has been extensively studied [5]. The presence of such azobenzene molecules in a liquid crystal environment brings out interesting effects, the principle behind which is outlined in the following. Upon uv irradiation (around 360 nm, corresponding to the π - π^* band of the azo group), the energetically more stable E configuration with an elongated rodlike molecular form, changes into the bent Z configuration. The reverse transformation can be brought about by illuminating with visible light (around 450 nm, corresponding to the n - π^* band). This latter change can also occur spontaneously in the “dark” by a process known as *thermal back relaxation*. The liquid crystalline phase is stabilized by the rodlike E form, but is destabilized by the bent Z form. Therefore, the E-Z change generally leads to a lowering of the phase transition temperature. The resulting photoinduced isothermal transition has been observed for a variety of systems exhib-

iting different phases [6–20]. Normally, the photoinduced phase will have higher point group symmetry although exceptions have been reported [21]. The influence of light on the magnitude of the polarization has been reported in the Sm- C^* [6,7,22–25], Sm- C_A^* [26], and banana-shaped $B2$ phases [27]. In this paper we report results of detailed investigations of the photoinduced effects on the electric polarization, tilt angle, response time, and rotational viscosity in the vicinity of the Sm-A–Sm- C_A^* transition.

II. EXPERIMENT

The compound 4-(1-trifluoromethylheptyloxy carbonyl) phenyl 4'-octyloxybiphenyl 4-carboxylate (TFMHPOBC), originally synthesized by Suzuki *et al.* [28], and exhibiting the Sm-A–Sm- C_A^* transition was used as the host and the photoactive guest compound was 4-(4-ethoxyphenylazo)phenyl hexanoate (EPH) having a nematic mesophase. The molecular structures of these two compounds are shown below.



All the measurements reported in this paper have been carried out on a mixture (referred to as mixture 1 hereafter) containing (1)5 wt % of EPH in TFMHPOBC. Polarizing microscopy observations showed that mixture 1 exhibits the sequence isotropic (Iso)–Sm-A–Sm- C_A^* . Electrical switching measurements, to be discussed later, confirm that the low-temperature mesophase is indeed Sm- C_A^* . The sample was contained between two indium tin oxide–coated glass plates having a polyimide layer to induce planar alignment of the

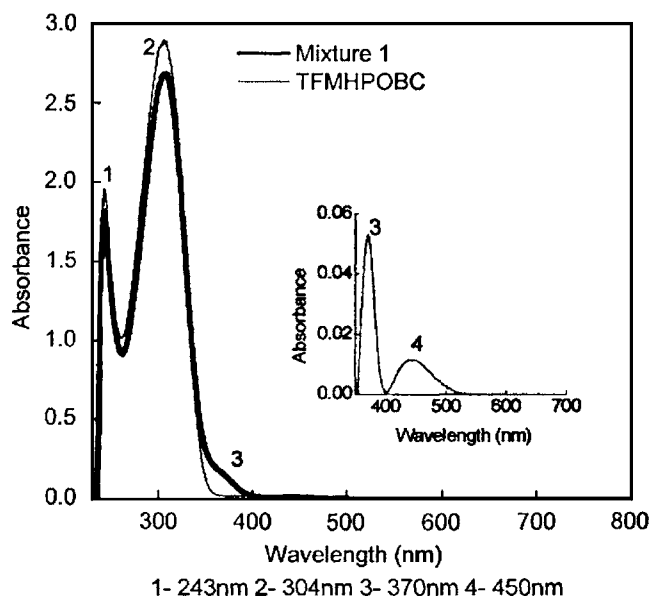


FIG. 1. Absorption spectra for pure TFMHPOBC (thin solid line) and mixture 1 containing 5% of EPH (thick solid line) obtained using 0.1 mM/l solutions with chloroform. The peaks labeled 1 and 2 are present in both materials and therefore do not participate in the photodriven phenomenon. In order to extract the absorption peaks appearing at higher wavelengths for mixture 1, the background due to peak 2 was subtracted out by a curve-fitting process which results in two clear absorption maxima to be seen at 370 and 450 nm (see inset) corresponding to the π - π^* transition of the E form and the n - π^* transition of Z isomers, respectively.

molecules. The cell gap, defined using Mylar strips, was $\sim 6 \mu\text{m}$.

The uv apparatus used for inducing photoisomerization consisted of an intensity-stabilized uv source (peak wavelength 365 nm) with a fiber-optic guide (Hamamatsu L7212-01, Japan) along with a uv bandpass filter (UG 11, Newport). An additional ir block filter was inserted just before the sample to prevent any effects of heat radiation from the uv source. The actual power (I_{uv}) of the radiation passing through the filter combination, falling on the sample was measured with a uv power meter (Hamamatsu, C6080-03) kept in the sample position. Electric polarization measurements have been carried out using the Diamant bridge technique [29] as well as the triangular wave method [30]. Electro-optic tilt angle data have been obtained using a mechanized stage for sample rotation by employing the low-frequency switching method [31].

III. RESULTS AND DISCUSSION

A. Absorption measurements

The absorption spectra for pure TFMHPOBC as well as for mixture 1 obtained using 0.1 mM/l concentration solutions, prepared using chloroform, taken in 1 cm path length quartz cells are shown in Fig. 1. The peaks at 243 nm (peak 1) and 304 nm (peak 2) are present in both the materials and thus must be arising due to the TFMHPOBC molecule, which per se is nonphotoactive and therefore we will

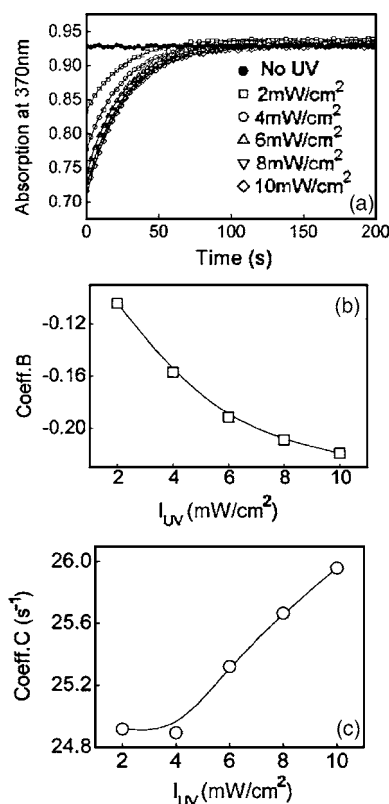


FIG. 2. Absorption data taken in the Sm-C_A^* phase at a constant wavelength of 370 nm as a function of time to show the recovery of the E form after different levels of the uv radiation (I_{uv}) illuminating the sample is switched off. (I_{uv} value increases from 0 for the topmost set to 10 mW/cm^2 for the bottom-most set in steps of 2 mW/cm^2 .) The solid line through the data representing Eq. (1) shows that the phenomenon can be described in terms of first order kinetics with the amplitude [coefficient B (b)] and the rate constant [coefficient C (c)] having a monotonic variation with I_{uv} .

not discuss these peaks anymore. The spectrum for mixture 1 shows two additional absorption maxima, one at 370 nm and the other at 450 nm, the latter being too weak to be seen on the scale shown. In order to depict in a clear fashion the peaks present at these wavelengths, we fitted the raw data to an expression containing two Gaussians and a background term due to the peak at 304 nm. The fit, after subtracting the background, is shown in the inset. The two peaks are associated with the π - π^* transition of the E form (at 370 nm, peak 3 in the inset of Fig. 1) and the n - π^* transition of Z isomers (at 450 nm, peak 4) of the EPH molecule.

The time dependence of the recovery of the E form after the illumination is turned off while the sample is being maintained in the Sm-C_A^* phase at 100 °C, is shown in Fig. 2(a). The qualitative trend observed for various values of I_{uv} appears to be the same. For a quantitative description, we fitted the data to a monoexponential rate law

$$A(t) = A_o + B \exp(- Ct) \tag{1}$$

where A_o is the final limiting value of the absorption reached and B the change in the absorption value with respect to the initial point. The coefficient C is a rate constant the inverse

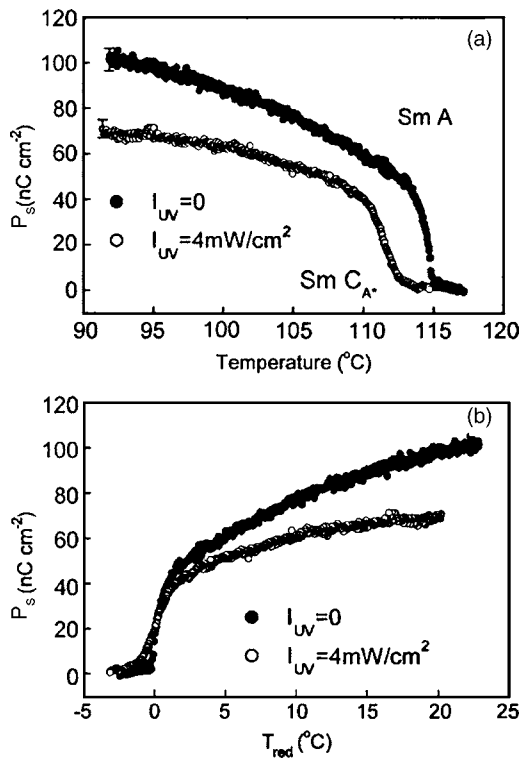


FIG. 3. (a) Temperature dependence of the spontaneous polarization (P_s) in the absence of uv (top curve) and when the sample is illuminated with $I_{uv}=4$ mW/cm² (bottom curve). Notice the reduction in the P_s value as well as a shift in the transition temperature for the uv-illuminated case. The diagram in (b) gives the same data but as a function of reduced temperature T_{red} , accounting for the shift in the transition temperature between the two cases. The lower value in P_s for the uv-illuminated case is considered to be the primary photoelectric effect (see text).

of which would be the characteristic time for the process. The solid lines in Fig. 2(a) show that this expression describes the data quite well for all the I_{uv} powers (2–10 mW/cm²) used in these experiments, indicating that the first order kinetics of the thermal back relaxation process of the EPH molecule is essentially unaltered even in the presence of the anisotropic layered environment. The amplitude of the change due to the uv illumination (coefficient B) and the inverse of the characteristic time (coefficient C) show a monotonic variation with I_{uv} [see Figs. 2(b) and 2(c)].

B. Temperature-dependent polarization measurements

In the antiferroelectric Sm-C_A* phase, application of triangular and sinusoidal wave fields to the sample yielded, respectively, a two-peak trace per half cycle of the applied field and a double hysteresis loop, features that are characteristic of the tristate switching expected for the phase. The combined area under the two-peak trace is a direct measure of spontaneous polarization (P_s). The temperature dependences of P_s obtained from such traces in the absence of the uv radiation and upon illuminating the sample with I_{uv} (magnitude of uv intensity) = 4 mW/cm² are shown in Fig. 3(a). The qualitative trend remains the same with and without UV, but

two distinguishing features seen in the presence of uv radiation are that there is a reduction in the transition temperature (T_c) by about 3 °C and that the saturated value of P_s achieved deep in the Sm-C_A* phase is about 30% lower as compared to that without uv illumination. The first feature is quite common in the area of photoinduced phase transitions [6–16], including the ones between layered phases [7,8,24,32] as in the present case. It may perhaps be argued that the reason for the shift in the transition temperature is due to local heating effects caused by the uv radiation. As mentioned earlier, we took precautionary steps to reduce (or eliminate) such a possible effect by introducing an ir block filter between the sample and the uv source. A further proof for the E-Z isomerization being the dominant feature and not the local heating was seen in the dielectric measurements, reported in the second part of these investigations: the temperature shift for the Iso–Sm-A transition is smaller (~ 0.9 °C for $I_{uv}=4$ mW/cm²) than that for the Sm-A–Sm-C_A* transition. For the second feature we use the explanation and model given by Langhoff and Giesselmann [33] to describe photoferroelectric effects. According to them, light (of a proper wavelength) influences the spontaneous polarization of a photoferroelectric material in two ways: the *primary* and *secondary* effects. The primary photoelectric effect (PPE) is associated with the change in P_s at a constant reduced temperature T_{red} ($=T_c-T$) owing to a change in the polar ordering and/or the transverse molecular dipole moment. The secondary photoelectric effect (SPE), on the other hand, is the change in P_s caused by the radiation-induced shift in T_c . To separate the two effects, the data in Fig. 3(a) are replotted as a function of reduced temperature [see Fig. 3(b)] by taking into account the transition temperature T_c (at the corresponding I_{uv} value). The presence of a strong PPE is evident from the diagram. Deep in the Sm-C_A* phase we observe a 30% reduction in the P_s value, which is much larger than the 11% change reported [33].

C. Temperature dependence of tilt angle

According to the authors of Ref. [33], in the Sm-C* phase, PPE is directly related to the change in the bilinear coupling coefficient, which is a measure of the coupling between the spontaneous polarization and the tilt angle that the molecules make with respect to the layer normal. In order to understand the influence of the nature of the polarization–tilt angle coupling we measured the optical tilt angle (θ) across the transition. The qualitative trend for the data collected in the absence of light and upon illuminating the sample with $I_{uv}=4$ mW/cm² is the same with a reduction in the transition temperature (T_c) upon uv illumination by the same magnitude as for the P_s data. In analogy with the photoferroelectric effect we can define a photoclinic effect for the light-induced change in the tilt angle. To separate the possible primary and secondary effects, the data are shown in Fig. 4 in terms of the reduced temperature. Notice that unlike P_s , there is no primary photoclinic effect and the difference in the behavior between the no uv and with uv data can be simply accounted for by a shift in the transition temperature. In other words, light does not, per se, alter the tilt angle of the system. A

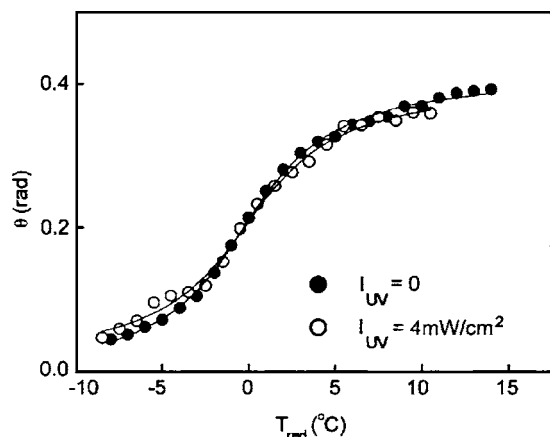


FIG. 4. Tilt angle (θ) variation as a function of reduced temperature T_{red} in the absence of uv (filled circles) and when the sample is illuminated with $I_{uv}=4$ mW/cm² (open circles).

similar result was observed by Langhoff and Giesselmann [33] at two discrete temperatures in the Sm-C* phase of a material exhibiting the Sm-C*–Sm-A transition. We shall discuss the qualitative analysis of the influence of light on the polarization-tilt coupling in a later section.

D. Temperature dependence of response time and rotational viscosity

The full width at half maximum (FWHM) of the current response peaks is a measure of the time taken by the system to switch from the equilibrium antiferroelectric to the ferroelectric state present when an electric field is applied. Figure 5 shows the temperature dependence of the response times in the absence of light and when $I_{uv}=4$ mW/cm² is shone on

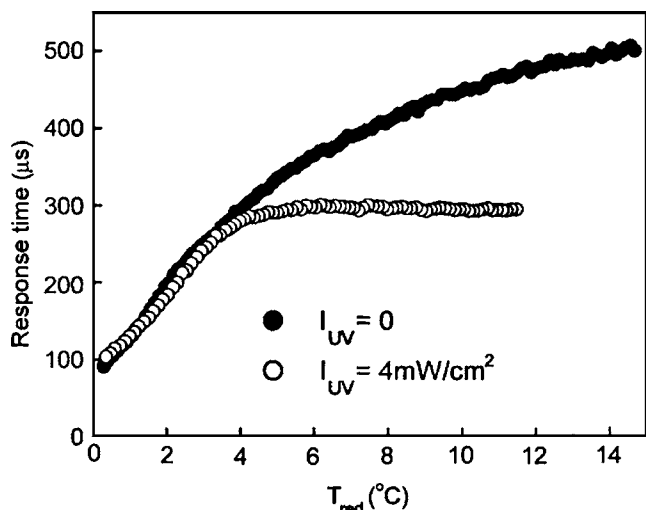


FIG. 5. Temperature dependence of the response time, associated with the time needed by the sample to switch between the antiferroelectric and the field-induced ferroelectric states, extracted from the FWHM of the current response traces in the absence of uv (filled circles) and when the sample is illuminated with $I_{uv}=4$ mW/cm² (open circles). The response becomes faster in the presence of the uv light.

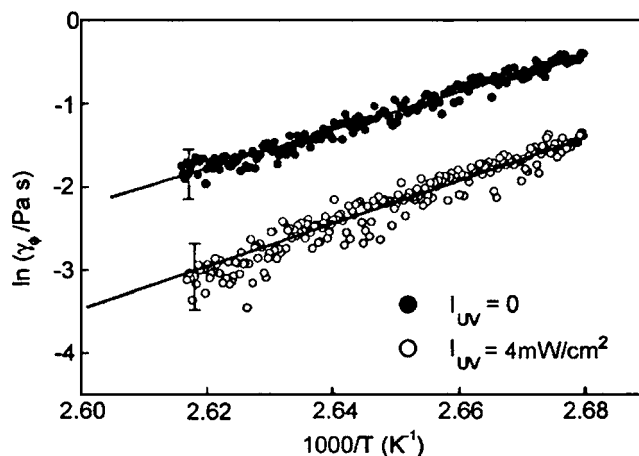


FIG. 6. Semilogarithmic plot of the temperature dependence of the rotational viscosity γ_ϕ without uv (filled circles) and in the presence of $I_{uv}=4$ mW/cm² (open circles); the γ_ϕ values were calculated using Eq. (2). While the absolute values are lowered by the uv illumination, the slope of the straight lines drawn through the data remains the same, indicating that the activation barrier height remains essentially unaltered.

the sample. (The positive curvature for the temperature dependence of the response time is a known feature; see Ref. [34].) It is seen that the response becomes faster in the uv-illuminated case. This seems to be a common feature with photoinduced transitions associated with a phase exhibiting polarization [27]. The features of the current response profile can be used to evaluate the rotational viscosity associated with the electrical switching process. For the triangular wave field used in these measurements, the rotational viscosity γ_ϕ associated with the azimuthal switching of the sample is given by [35]

$$\gamma_\phi = \frac{AP_s^2 E_{max}}{I_{max}} \tag{2}$$

where A is the area of the sample cell, I_{max} is the peak current, and E_{max} is the corresponding applied field at that instant. The temperature dependence of γ_ϕ in the no-uv and with-UV situations is shown in Fig. 6 and it is observed that in the presence of uv the system exhibits a substantially lower viscosity. The presence of Z isomers with their bent form (as opposed to the rigid rodlike E form) contributes to lowering the viscosity of the system perhaps due to a possible reduction in the orientational ordering of the overall medium. A second and more plausible reason could be that the reduction is due to lowering of P_s in the presence of the uv radiation. The temperature dependence of γ_ϕ with and without uv illumination seems to be the same, as indicated by the slope of a straight line fitted to the data. The slope is a measure of the activation energy, which turns out to be 170 kJ/mol, somewhat higher than commonly observed for ferroelectric liquid crystals [4].

E. Analysis of polarization-tilt coupling

The starting point for this analysis is the drastically different behaviour of the thermal variation of P_s and θ upon uv

illumination, presented in Secs. III B and III C. Whereas θ has no primary photoclinic effect, P_s exhibits a significant primary photoferroelectric effect. Thus at a fixed reduced temperature, the P_s/θ ratio decreases upon uv illumination. Since the nature of the P_s - θ coupling has been elaborately studied in the case of the Sm- C^* phase, we employ those models [36–38] for the present case. The fundamental basis for these models is the feature that the transition from the Sm-A phase to the Sm- C^* (or Sm- C_A^*) phase is brought about by the tilting of the molecules and not by a specific ordering of their transverse dipoles. Thus the tilt angle θ is the primary order parameter and the spontaneous polarization P_s a secondary order parameter. In a simple-minded picture [36], P_s and θ are coupled in a linear fashion and the Landau free energy for a helix-free system is written as

$$F = F_o + \frac{a}{2}\theta^2 + \frac{b}{4}\theta^4 + \frac{P^2}{2\chi} - CP\theta - PE. \quad (3)$$

Here F_o is the nonsingular part of F , $a [= \alpha(T - T_c)]$ and b are the Landau coefficients, χ is the high-frequency dielectric susceptibility, and E is the applied electric field, which when equal to zero leads to $P = P_s$. Notice that the coupling between P and θ is done through the bilinear coupling coefficient C and that the P_s/θ ratio is a constant. Even early experiments showed that although the P_s/θ ratio is weakly dependent on temperature far away from the transition, it varies strongly on approaching the Sm-A phase from below. In order to explain such a discrepancy an extended mean-field model, usually referred to as the “generalized mean-field model” (GMF) was proposed [37]. This model incorporated a sixth order term in θ to account for the possibility of first order transition and a concomitant tricritical point [39]. More importantly it introduced a biquadratic coupling term $-\Omega P^2 \theta^2/2$ to bring in transverse quadrupolar ordering, which is nonchiral in character and amplifies the spontaneous polarization. In the absence of certain terms that were introduced purely for stability reasons or for explaining the temperature variation of the helical pitch, the model is written as

$$F = F_o + \frac{a}{2}\theta^2 + \frac{b}{4}\theta^4 + \frac{c}{6}\theta^6 + \frac{P^2}{2\chi} - CP\theta - \frac{\Omega}{2}P^2\theta^2 - PE \quad (4)$$

and yields a simple relation between P and θ (see also [40]):

$$P = \frac{C\theta}{1/\chi - \Omega\theta^2}. \quad (5)$$

In this model an all-important parameter $\beta \propto C/\Omega$ was considered, whose value governs the temperature dependence of the P_s/θ ratio.

To provide a microscopic meaning to the quadrupolar ordering mentioned above, a microscopic model [38,41] was proposed based on a single particle potential. The main assumption in this model is that the ordering of the transverse electric dipoles (of moment μ) is induced by the hindered rotation of the tilt of the molecules. The orientation of the

dipoles in the plane perpendicular to the long molecular axis is defined by an angle ψ and the single particle potential is given by

$$U(\psi) = -a_1\theta \cos \psi - a_2\theta^2 \cos 2\psi. \quad (6)$$

The first term on the right is of chiral character and is analogous to the bilinear coupling term and the second term compares with the biquadratic coupling term of the GMF model. The microscopic model expects that the relation $a_1\theta \ll a_2\theta^2$ is valid since chiral interactions are supposed to be weak except in the vicinity of T_c . Using Boltzmann statistics, Meister and Stegemeyer [41] obtained

$$P = \frac{A_1}{T}\theta + \frac{A_1A_2}{T^2}\theta^3. \quad (7)$$

To compare this expression with that from the GMF model [Eq. (5)], which is phenomenological in nature, Eq. (5) was expanded in a Taylor series in θ [40]. Neglecting higher-order terms the expanded form can be written as

$$P = \chi C\theta + \chi^2 C\Omega\theta^3. \quad (8)$$

It may be noted that based on a phenomenological model Beresnev *et al.* [42] had predicted such a cubic equation, which successfully describes the P_s - θ relation for quite a few compounds [43]. With the help of Eqs. (7) and (8), the GMF coefficients C and Ω can be written in terms of the A_1 and A_2 coefficients of the microscopic model and after some algebra a simple form of the θ dependence of polarization is written as

$$P = \frac{A_1\theta}{T - A_2\theta^2}. \quad (9)$$

With this information in the background let us now look at the influence of the uv illumination on the P_s - θ coupling. The P_s vs θ data in the absence of and upon uv illumination are given in Fig. 7(a). The figure also shows the fitting done using expressions (5) and (9), which are virtually indistinguishable from each other in the diagram and both describe the data very well. Perhaps the indistinguishable feature should not be surprising since the two equations have very similar form except for the temperature parameter in Eq. (9). The striking feature to be noted is that while the no-uv data have a significant curvature, the data obtained under uv illumination are highly linear (in fact, a fit done to the expression for a straight line yields only a slightly lower-quality fit). The coefficients C and Ω of the GMF model were found to be $(4.4 \pm 0.1) \times 10^7 \text{ V m}^{-1}$, $(8.2 \pm 0.4) \times 10^{10} \text{ N m}^2 \text{ C}^{-2}$ for the no-uv data set and $(5.2 \pm 0.2) \times 10^7 \text{ V m}^{-1}$, $(1.8 \pm 0.1) \times 10^{10} \text{ N m}^2 \text{ C}^{-2}$ for the data with uv illumination. These values are of the same order of magnitude as for other ferroelectric liquid crystals [37]. The coefficients A_1 and A_2 of the microscopic model are $0.51 \pm 0.01 \text{ C K m}^{-2}$, $1105 \pm 43 \text{ K}$ and $0.59 \pm 0.02 \text{ C K m}^{-2}$, $319 \pm 125 \text{ K}$ for the no-uv and with-uv cases. It is seen that in the case of the GMF as well as the microscopic models the chiral coefficients (C and A_1) increase slightly ($\sim 17\%$) upon uv illumination. In contrast the nonchiral coefficients (Ω and A_2) show a large change, decreasing by a factor of 4. In other words, uv illumination

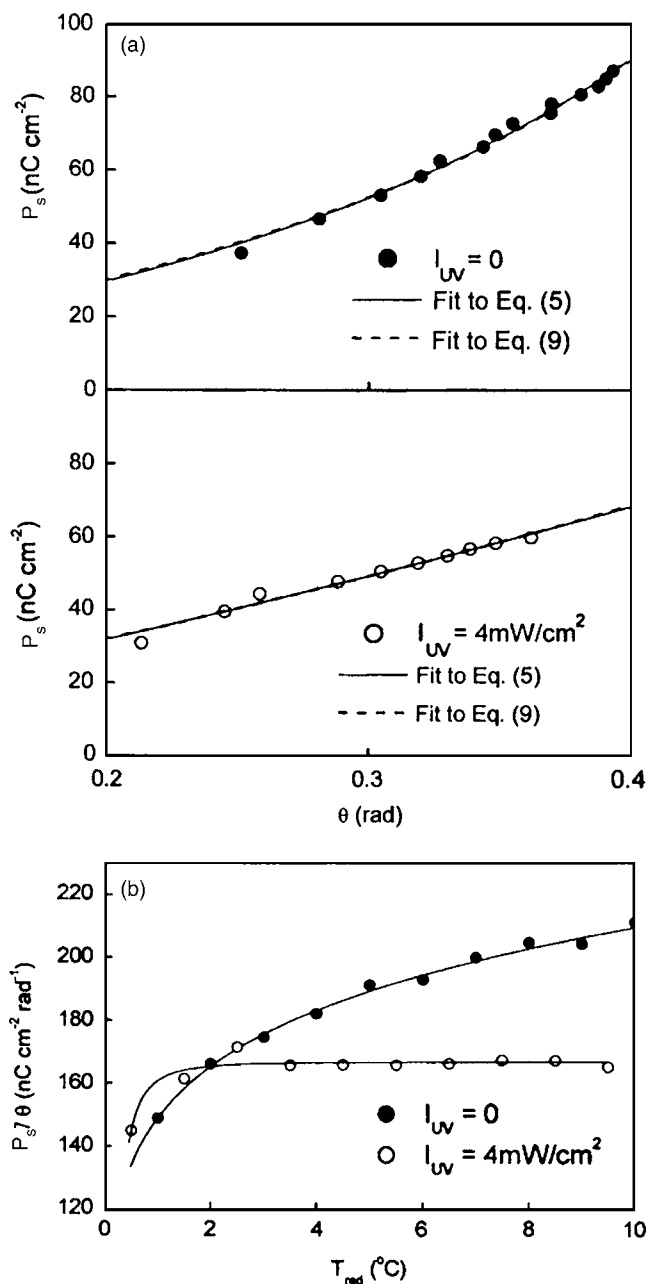


FIG. 7. (a) Tilt angle dependence of polarization in the absence of uv (top panel) and upon shining uv (bottom panel). Notice that the no-uv data have a significant curvature, whereas the data obtained with uv are nearly linear. The fits to Eqs. (5) and (9) are shown as solid and dashed lines, respectively. (b) Temperature dependence of the P_s/θ ratio for the no-uv and with-uv conditions. The former has a variation with temperature throughout the range shown, whereas under uv illumination the ratio is nearly constant except near the transition. The solid lines are meant as guides to the eye.

reduces the nonchiral aspect of the P_s - θ coupling, thus supporting the qualitative change in the behavior of the P_s vs θ data from nonlinear trend to a linear one as shown in Fig. 7. As mentioned earlier according to the GMF model, the value of $\beta \propto C/\Omega$ governs the temperature dependence of the P_s/θ ratio. This value increases from 5.4×10^{-4} to 28.4

$\times 10^{-4} \text{ C m}^{-2}$ upon uv illumination, i.e., an increase of a factor of 5. Since the value of β changes between 0 and 1 in the model (that incorporates additional terms for stability reasons as well as to account for pitch variation but which are not important from the viewpoint of present studies) such a large variation means that there should be a substantial change in the thermal behavior of the P_s/θ ratio. Figure 7(b) shows this to be indeed true: for the no-UV case the ratio varies over the entire temperature range of measurement, but the data collected with uv remain essentially constant except in the vicinity of the transition. This is in accordance with the predictions of the GMF model (see, for example, Fig. 12 of Ref. [37]).

Having observed that uv illumination increases the ratio of the chiral to achiral coupling terms, the question raises as to the origin of such a feature. Three points that must be remembered here are (i) the value of polarization decreases upon illumination, (ii) the photoactive dopant employed in these studies is a nonchiral compound, and (iii) the photoactive molecule has a rodlike shape in the absence of uv illumination, but assumes a bent shape when illuminated. It may also be recalled that earlier measurements in ferroelectric [6,7,23–25] as well as antiferroelectric [26] systems have also found that with photoactive azobenzene molecules, uv illumination always leads to a lowering of the value of P_s . The decrease of P_s in the presence of light looks surprising since a strongly asymmetric (bent) form of the Z isomer of EPH having a large dipole moment (3 D) [44] as compared to the E form (0.1 D) should have resulted in an increase in P_s . One possible reason could be the most commonly observed lowering of the transition temperature. This appears to be the case in, for example, reports of Refs. [6,7,25]. In the present studies this cause can be ruled out as the reduced temperature plots (in which the shift in the transition temperature is accounted for) also retain this feature (Fig. 3). A second possibility is that a nanophase separation, similar to that described by Lansac *et al.* [45], takes place, expelling the bent EPH molecules to a segregated layer between two smectic layers composed of the host molecules. Since bend directions of the EPH molecule in the segregated layer could be random and there is an apparent increase in the volume of the system with a consequential reduction in the dipole moment per volume, the measured P_s would be lower than before uv illumination. However, in x-ray measurements in systems having EPH or similar azobenzene molecule, upon uv illumination the maximum observed increase in layer spacing is quite small ($\sim 0.05 \text{ nm}$) (see, e.g., Ref. [27]). The resulting volume change due to this increase in layer spacing would be only 1% of the actual volume. Consequently, the decrease in dipole moment/unit volume and therefore P_s should be of the same order, but the measured P_s decrease is much larger (30%). Also to be recalled is that in the studies of Komitov *et al.* [24], the Z isomer of the photoactive molecule used has a linear shape and that with thioindigo molecules [23] the P_s value increases upon light illumination. Thus, in these cases as well as that of the present study, the nanophase segregation mechanism appears to be a less probable cause for the light-induced changes in P_s . To explain the various observations mentioned above we put forth the following argument, on the lines of the guest-host effect of P_s

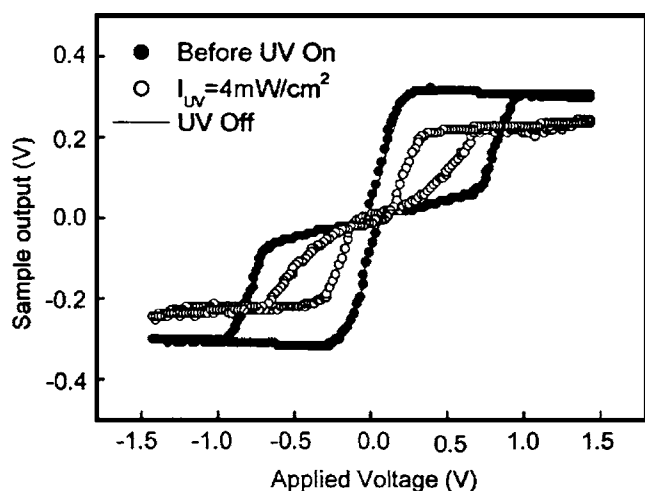


FIG. 8. Hysteresis loops obtained before uv illumination (filled circles) and with $I_{uv}=4 \text{ mW/cm}^2$ (open circles). When the uv illumination is turned off, the system recovers the original state completely and the data essentially coincide with those obtained before uv illumination. This set is shown as a line.

in induced Sm- C^* phases [41]. The argument is based on the mutual steric interactions and consequent mutual orientation directions of the steric dipoles of the guest photoactive molecules and the host nonphotoactive molecules. Such an interaction may not in every case make the dipole moment direction of the guest molecule to be coincident with those of the host molecules, but might rotate it by a certain azimuthal angle. Depending on the value of the azimuthal angle, the guest dipole moment could have either an additive (if parallel to the host dipole) or a subtractive (if perpendicular, i.e., lying in the tilt plane) component along the direction of the host dipole moment. It should be recalled that, particularly in the case of azobenzenes (say, EPH), the Z isomer has a large dipole moment. Therefore it is possible that in the present case, the dipole of the Z isomer of EPH makes a substantial angle with respect to the host dipole (of TFMHPOBC), resulting in a substantial reduction in the value of P_s upon uv illumination.

F. Temporal measurements of polarization

Figure 8 shows the hysteresis loops obtained at a constant temperature of 102°C in the Sm- C_A^* phase, before, during the process of illumination with uv radiation as well as after switching the radiation off; the last mentioned measurements were done by keeping the sample in the dark. As is to be expected, uv radiation causes the loop size to shrink. More importantly, when the radiation is switched off, the process is reversed and the original P_s value is recovered. (The current response traces obtained show similar features in the presence and absence of uv.) The decrease and the recovery in P_s are highly reproducible and can be repeatedly observed by turning the radiation on and off, confirming that the effects are photostimulated, and caused by E-Z conformational change and the thermal back relaxation of the EPH molecules. The temporal variation of P_s at three different temperatures in the Sm- C_A^* phase is shown in Fig. 9. Turning the

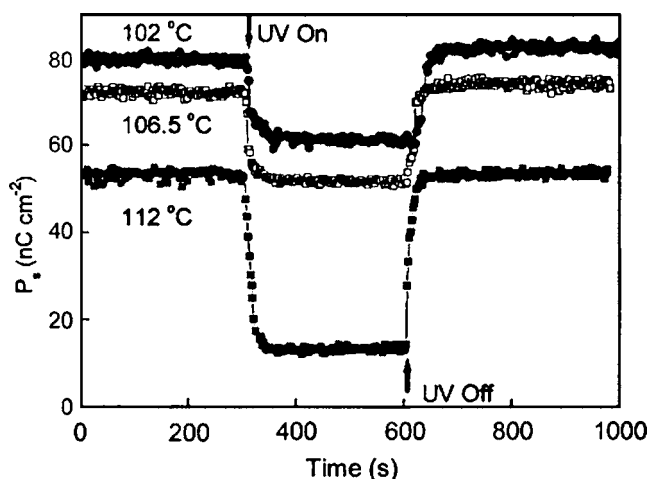


FIG. 9. Time dependence of P_s upon uv illumination ($I_{uv}=4 \text{ mW/cm}^2$) and subsequent switch off, at three different temperatures in the Sm- C_A^* phase. The change in P_s is very large at temperatures close to T_c of the unilluminated sample. At each temperature the time required to achieve the photostationary value upon uv on, as well as to recover the original value when the uv is switched off, seems to be comparable.

radiation on, the value of P_s initially decreases rapidly and settles to a photostationary state within about 35 s. When the radiation is switched off and the sample is left in the dark, the reverse process takes place with P_s increasing rapidly first and slowing down later, but recovering the original P_s value that existed before uv irradiation. Surprisingly the time involved for this thermal process seems to be not very different from that for the UV-on photochemical process. Generally this thermal process takes place on a substantially longer time scale [12]. Another feature to be noted in the data of Fig. 9 is that the photoinduced change in P_s is instantaneous, i.e., it does not involve any delay between the instant at which the uv is switched on or off and the time at which the system responds. This is in contrast to the long delay times observed especially in the case of the photoinduced nematic-isotropic transition [14]. A possible reason for observing faster thermal process and the absence of delay times in the present case could be that the phases involved on both sides of transition possess a layer structure and that the change that occurs is confined to in-plane rotation (change of tilt) of the molecules. The argument is supported by the fact that a similar feature was observed in another case wherein the two phases involved have a layer structure [32]. On a structural level, since the shape change of EPH happens in the core region of the molecule, it will change the mutual interaction between the rigid core part of the guest and host molecules and their aliphatic parts. If the photoinduced transition is from the nematic to isotropic, the bent azobenzene molecules can occupy sites where their rigid core is away from the core region of the host molecules, since such a translation along the director direction is permitted by the system. Therefore, the driving force to return to the equilibrium situation upon switching off the radiation is small and consequently the thermal back relaxation dynamics is slow. In the case of the transition involving two layered phases

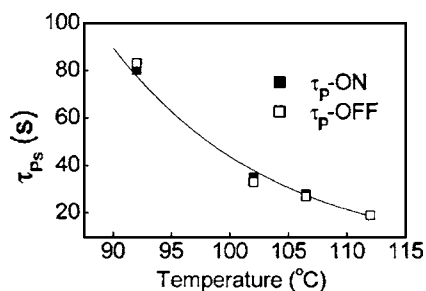


FIG. 10. Temperature dependence of the time required for the polarization to achieve the photostationary value (τ_p on, filled squares) and to regain the original value (τ_p off, open circles). The solid line is a fit to the Arrhenius expression yielding an activation energy value of 86 kJ/mol.

such a sliding of the azobenzene molecules to regions away from the core region of the host molecules is not permitted. Hence, if the nanophase segregation does not take place, the bent azobenzene molecules will be forced to stay inside the host layer creating a frustrated situation. This perhaps increases the magnitude of the driving force for a quick restoration of the pre-UV situation when the radiation is turned off resulting in a faster thermal back relaxation process.

Further, the photodriven change in P_s is very large when the temperature at which the irradiation is done is close to the transition to the Sm-A phase (see the data for 112 °C in Fig. 9). In the usual thermally driven phase transition case, the temperature derivative of P_s is taken as a measure of the pyroelectric coefficient [46]. In a similar fashion we take the derivative of P_s with time to define the photoferroelectric coefficient and realize that high values of such a coefficient can be realized by uv illuminating the sample at temperatures close to T_c . Perhaps this property can be exploited to con-

struct uv-light sensors with the advantage that the response is quite fast.

The temperature dependence of the time taken for the P_s value to change to the photostationary value upon uv illumination (τ_p on) and for regaining the initial value after the uv is turned off (τ_p off) is shown in Fig. 10. As already stated the magnitudes of the two parameters are comparable with each other and they are also comparable to the data collected from absorption measurements of the time involved for the E-Z to Z-E isomerization to take place confirming further that the P_s change is to a large extent associated with the isomerization processes and not local heating. The temperature dependence of the τ_p parameters can be described by an Arrhenius equation of the type $\tau_p \sim \exp(-W/kT)$, where k is the Boltzmann constant, T is the absolute temperature, and W is the activation energy. The calculated W value is 86 kJ/mol and is comparable to that seen for the relaxation modes associated with the Sm-A–Sm- C_A^* transition [47].

In summary, we have investigated the photoinduced effects on the electric polarization, tilt angle, response time, and rotational viscosity in the vicinity of the Sm-A–Sm- C_A^* transition of a system comprising photoactive guest and non-photoactive host molecules. The studies bring out the presence of both the primary and secondary photoferroelectric effects in the Sm- C_A^* phase. The data have been compared with the predictions of the generalized mean-field and microscopic models.

ACKNOWLEDGMENTS

We gratefully acknowledge the financial support by the Department of Science and Technology, New Delhi, under a SERC project (Grant No. 93357).

-
- [1] See, e.g., S. Chandrasekhar, *Liquid Crystals*, 2nd ed., (Cambridge University Press, Cambridge, U.K., 1992).
- [2] R. B. Meyer, L. Liebert, L. Strzelecki, and P. Keller, *J. Phys. (Paris)*, Lett. **36**, L69 (1975).
- [3] A. D. L. Chandani, E. Gorecka, Y. Ouchi, H. Takezoe, and A. Fukuda, *Jpn. J. Appl. Phys., Part 2* **28**, L1265 (1989).
- [4] For reviews on the antiferroelectric and sub phases, see S. T. Lagerwall, *Ferroelectric and Antiferroelectric Liquid Crystals* (Wiley-VCH, Weinheim, 1999); I. Musevic, R. Blinc, and B. Zeks, *The Physics of Ferroelectric and Antiferroelectric Liquid Crystals* (World Scientific, Singapore, 2000).
- [5] See, e.g., H. Rau, in *Photochemistry and Photophysics*, edited by J. F. Rabek (CRC Press, Boca Raton, FL, 1989), Vol. II.
- [6] T. Ikeda, T. Sasaki, and K. Ichimura, *Nature (London)* **361**, 428 (1993).
- [7] H. J. Coles, H. G. Walton, D. Guillon, and G. Poetti, *Liq. Cryst.* **15**, 551 (1993).
- [8] S. Servaty, F. Kremer, A. Schonfeld, and R. Zentel, *Z. Phys. Chem.* **190**, 73 (1995).
- [9] C. H. Legge and G. R. Mitchell, *J. Phys. D* **25**, 492 (1992).
- [10] C. Sánchez, R. Alcalá, S. Hvilsted, and P. S. Ramanujam, *J. Appl. Phys.* **93**, 4454 (2003).
- [11] N. Tamaoki, *Adv. Mater. (Weinheim, Ger.)* **13**, 1135 (2001).
- [12] G. G. Nair, S. K. Prasad, and C. V. Yelamaggad, *J. Appl. Phys.* **87**, 2084 (2000).
- [13] S. Krishna Prasad, K. L. Sandhya, Geetha G. Nair, Uma S. Hiremath, and C. V. Yelamaggad, *J. Appl. Phys.* **92**, 838 (2002).
- [14] Geetha G. Nair, S. Krishna Prasad and Gurumurthy Hegde, *Phys. Rev. E* **69**, 021708 (2004).
- [15] S. Krishna Prasad, Geetha G. Nair, K. L. Sandhya, and D. S. Shankar Rao, *Curr. Sci.* **86**, 815 (2004).
- [16] Gurumurthy Hegde, Geetha G. Nair, S. Krishna Prasad, and C. V. Yelamaggad, *J. Appl. Phys.* **97**, 093105 (2005).
- [17] V. Ajay Mallia, Mathew George, and Suresh Das, *Chem. Mater.* **11**, 207 (1999).
- [18] H. Knobloch, H. Orendi, M. Buchel, T. Seki, S. Ito, and W. Knoll, *J. Appl. Phys.* **77**, 481 (1995).
- [19] L. M. Blinov, M. V. Kozlovsky, M. Ozaki, K. Skarp, and K. Yoshino, *J. Appl. Phys.* **84**, 3860 (1998).
- [20] M. Eich, B. Reck, H. Ringsdorf, and J. H. Wendorff, *Proc. SPIE* **682**, 93 (1986).

- [21] S. Krishna Prasad and Geetha G. Nair, *Adv. Mater. (Weinheim, Ger.)* **13**, 40 (2001).
- [22] L. M. Blinov, M. V. Kozlovsky, M. Ozaki, and K. Yoshino, *Mol. Cryst. Liq. Cryst. Sci. Technol., Sect. C* **6**, 235 (1996).
- [23] L. Dinescu, K. E. Maly, and R. P. Lemieux, *J. Mater. Chem.* **9**, 1679 (1999).
- [24] L. Komitov, C. Ruslim, and K. Ichimura, *J. Nonlinear Opt. Phys. Mater.* **9**, 151 (2000).
- [25] A. Langhoff and F. Giesselmann, *ChemPhysChem* **3**, 424 (2002).
- [26] K. Shirota and I. Yamaguchi, *Jpn. J. Appl. Phys., Part 2* **36**, L1035 (1997).
- [27] Geetha G. Nair, S. Krishna Prasad, Uma S. Hiremath, and C. V. Yelamagadda, *J. Appl. Phys.* **90**, 48 (2001).
- [28] Y. Suzuki, T. Hagiwara, I. Kawamura, N. Okamura, T. Kitazume, M. Kakimoto, Y. Imai, Y. Ouchi, H. Takezoe, and A. Fukuda, *Liq. Cryst.* **6**, 167 (1989).
- [29] H. Diamant, K. Drenck, and R. Pepinsky, *Rev. Sci. Instrum.* **28**, 30 (1957).
- [30] K. Miyasato, S. Abe, H. Takezoe, A. Fukuda, and E. Kuze, *Jpn. J. Appl. Phys., Part 2* **22**, L661 (1983).
- [31] B. R. Ratna, S. Krishna Prasad, J. Naciri, P. Keller, and R. Shashidhar, *Ferroelectrics* **148**, 425 (1993).
- [32] S. Krishna Prasad, K. L. Sandhya, D. S. Shankar Rao, and Y. S. Negi, *Phys. Rev. E* **67**, 051701 (2003).
- [33] A. Langhoff and F. Giesselmann, *J. Chem. Phys.* **117**, 2232 (2002).
- [34] See, e.g., M. R. De La Fuente, A. Ezkurra, and M. A. Pérez-Jubindo, *Liq. Cryst.* **7**, 51 (1990); S. Krishna Prasad, S. M. Khened, S. Chandrasekhar, B. Shivkumar, and B. K. Sadasivha, *Mol. Cryst. Liq. Cryst.* **182B**, 313 (1990); A. Kocot, R. Wrzalik, J. K. Vij, and R. Zentel, *J. Appl. Phys.* **75**, 728 (1994); It may also be mentioned that a theoretical analysis even expects a power-law dependence; see K. Sarp, *Ferroelectrics* **84**, 119 (1988).
- [35] C. Escher, T. Geelhaar, and E. Bohm, *Liq. Cryst.* **3**, 469 (1988).
- [36] S. A. Pikin and V. L. Indenbohm, *Sov. Phys. Usp.* **21**, 487 (1979).
- [37] T. Carlsson, B. Zeks, C. Filipic, A. Levstik, and R. Blinc, *Mol. Cryst. Liq. Cryst.* **163**, 11 (1988).
- [38] B. Zeks, T. Carlsson, C. Filipic, and B. Urbanc, *Ferroelectrics* **84**, 3 (1988).
- [39] C. C. Huang and J. M. Viner, *Phys. Rev. A* **25**, 3385 (1982).
- [40] F. Giesselmann and P. Zugenmaier, *Phys. Rev. E* **52**, 1762 (1995).
- [41] R. Meister and H. Stegemeyer, *Ber. Bunsenges. Phys. Chem.* **97**, 1242 (1993).
- [42] L. A. Beresnev, E. P. Pozhidayev, and L. M. Blinov, *Ferroelectrics* **59**, 1 (1984).
- [43] S. K. Prasad and G. G. Nair, *Mol. Cryst. Liq. Cryst.* **202**, 91 (1991); Geetha G. Nair, Ph.D thesis Bangalore University, 1992 (unpublished).
- [44] V. Borisenko, D. C. Burns, Z. Zhang, and G. A. Woolley, *J. Am. Chem. Soc.* **122**, 6364 (2000).
- [45] Y. Lansac, M. A. Glaser, N. A. Clark, and O. D. Lavrentovich, *Nature (London)* **398**, 54 (1999).
- [46] See, e.g., J. Ruth, B. R. Ratna, J. Naciri, R. Shashidhar, S. K. Prasad, D. S. Shankar Rao, and S. Chandrasekhar, *Proc. SPIE* **1911**, 104 (1993).
- [47] H. Moritake, M. Ozaki, and K. Yoshino, *Jpn. J. Appl. Phys., Part 2* **32**, L1432 (1993).